Analysis of Dyakonov surface waves existing at the interface of an isotropic medium and a conductor-backed uniaxial slab

Sipeng Chen,[1] Zhongxiang Shen,[2,*] and Wen Wu[1]

[1]*Ministerial Key Laboratory of JGMT, Nanjing University of Science and Technology, Nanjing 210094, China*
[2]*School of Electrical and Electronic Engineering, Nanyang Technological University, Singapore 639798*
**Corresponding author: ezxshen@ntu.edu.sg*

Received March 10, 2014; revised June 19, 2014; accepted July 12, 2014;
posted July 21, 2014 (Doc. ID 207924); published August 7, 2014

In this paper, Dyakonov surface waves (Dyakonov SWs) existing at the interface between a semi-infinite isotropic medium and a conductor-backed uniaxial slab are analyzed with the help of an exponential-matrix method. The boundary conditions at the interface are formulated using eigenvalues and eigenvectors of two partnering media. Based on this, the existence region of Dyakonov SWs is formulated and proven to be highly dependent on the thickness of the uniaxial slab. Some relevant characteristics of the propagating Dyakonov SWs, such as the distribution of the propagation constant, and the electric- and magnetic-field distributions, are introduced and investigated. In addition, this method can be applied to analyze other finite thickness structures.

OCIS codes: (160.1190) Anisotropic optical materials; (240.6690) Surface waves; (350.5500) Propagation.
http://dx.doi.org/10.1364/JOSAA.31.001923

1. INTRODUCTION

Surface waves existing at the interface of two different media have been known for many years [1]. With the property of propagating at the interface and transversely attenuating while traveling away from the interface in an exponential form, surface waves have continuously attracted lots of attention. In 1988, Dyakonov [2] initially proved that a new special type of surface wave could exist at the interface of a lossless isotropic medium and a uniaxial birefringent medium within a certain angle range. These surface waves feature a hybrid nature and have the unique property of lossless propagation at the interface.

After that, Dyakonov surface waves (Dyakonov SWs) that were mostly caused by the symmetry differences of two partnering materials became an extensively researched topic. Averkiev and Dyakonov [3] analyzed the case in which Dyakonov SWs exist at the interface of two identical uniaxial media, where the optic axes of both media were located at the same interface but along different directions. Walker *et al.* [4] rigorously proved that Dyakonov SWs could also exist at the interface of isotropic–uniaxial (arbitrarily oriented) or isotropic–biaxial structures by using an exponential-matrix method, which was introduced by Morgan *et al.* in 1987 [5].

Later, Polo *et al.* made remarkable contributions to the intensive studies of Dyakonov SWs. They demonstrated that these surface waves could exist at the interfaces of many structures, such as uniaxial–uniaxial (the optic axes have tilted angles with the interface plane) [6], biaxial–biaxial [7,8], isotropic–electro-optic material [9], and isotropic–columnar thin film [10]. On the basis of previous research works [2–11], Takayama *et al.* successfully observed Dyakonov SWs for the first time with an Otto–Kretschmann configuration and confirmed the existence of these surface waves [12]. Afterward, they continuously conducted a lot of investigations, such as exploring the important role that Dyakonov SWs played in light transmission [13], proving that Dyakonov SWs could exist in multilayer metamaterial structures [14], and analyzing the coupling between plasmons and Dyakonov SWs [15].

For most papers mentioned above, the investigations were focused on structures that have infinite length in both directions normal to the interface. In fact, the study of Dyakonov SWs supported at the critical surface of a finite medium has more practical relevance in engineering applications. It is inevitable to make a trade-off between good performance and a tolerable thickness. Although the existence of the cut-off thickness at diverse dielectric slabs has been observed by researchers [11,15–20], for Dyakonov SWs, the related theoretical analysis has not been systematically introduced yet. It is necessary to derive the related characteristic equations and expressions, which can be used to analyze Dyakonov SWs existing at finite thickness structures.

This paper presents a theoretical analysis of Dyakonov SWs, which exist at the interface of a semi-infinite isotropic medium and a conductor-backed uniaxial slab. The obtained dispersion equation demonstrates that a tolerable thickness must be above a certain value if Dyakonov SWs are supported in this structure. A relevant equation is derived to calculate the minimum thickness value. After that, a numerical example is shown to illustrate the effect of the slab height on other key parameters that are closely interrelated with the existence of Dyakonov SWs. The distribution of the propagation constant in the existence region and the transverse electric-field distributions of both media are also given in this paper. Moreover, this method is generalized to discuss the existence state of Dyakonov SWs in other similar finite structures, such as

arbitrarily oriented uniaxial cases, combinations of different layered structures, and real conductor cases.

The organization of this paper is as follows. In Section 2, the dispersion equation of Dyakonov SWs supported by a conductor-backed slab is obtained by using a full wave analysis in this kind of structure. Section 3 presents some numerical results and discussion, including the angular existence domain, field distributions, and Dyakonov SWs existing at other finite thickness structures. Finally, conclusions are summarized in Section 4.

2. THEORETICAL FORMULATION

A. Full Wave Analysis of a Conductor-Backed Structure

The geometry being analyzed is shown in Fig. 1, where surface waves are supported at the interface ($z = 0$ plane) of two different media. The upper region ($z > 0$) is a semi-infinite medium A, while the lower region ($-d < z < 0$) is a finite medium B. The plane of $z = -d$ is considered as a perfect electric conductor (PEC) plane, which means that the tangential components of the electric field must be zero at the lower surface of medium B. In order to investigate the existence conditions of surface waves, an exponential-matrix method, which can be used to solve the boundary condition problems effectively [4,5,21–23], is applied in this paper.

Morgan *et al.* [5] have shown that, for an arbitrary source-free medium, the electric and magnetic fields tangential to the interface plane satisfy

$$\frac{d}{dz}\mathbf{S}(z) = -j\bar{\bar{T}}\cdot\mathbf{S}(z), \tag{1}$$

where $\mathbf{S}(z) = (E_x \quad E_y \quad \eta_0 H_x \quad \eta_0 H_y)^T$ is a column vector for the transverse fields, η_0 is the wave impedance of free space, and $\bar{\bar{T}}$ is a 4×4 coefficient matrix, which is given in Appendix A. Both the transverse electric and magnetic fields in Eq. (1) have an $\exp[j(\omega t - px)]$ dependence, where ω is the angular frequency, and p is the propagation constant along the $+x$ direction. In a homogeneous medium, a general solution of Eq. (1) can be written as a combination of eigenvalues and eigenvectors and is in the form of

$$\mathbf{S}(z) = [\mathbf{a}_1 \ \mathbf{a}_2 \ \mathbf{a}_3 \ \mathbf{a}_4] \begin{bmatrix} \exp(-j\lambda_1 z) & & & \\ & \exp(-j\lambda_2 z) & & \\ & & \exp(-j\lambda_3 z) & \\ & & & \exp(-j\lambda_4 z) \end{bmatrix} \begin{bmatrix} D_1 \\ D_2 \\ D_3 \\ D_4 \end{bmatrix}, \tag{2}$$

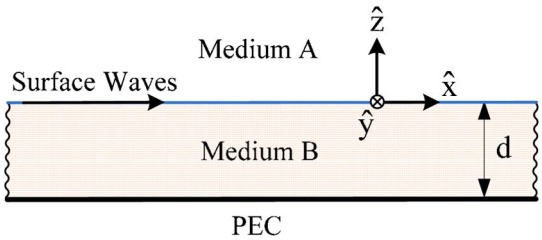

Fig. 1. Geometry of the structure considered. Surface waves are supported at the interface of two different media, propagating along the $+x$ axis.

where λ_n and $\mathbf{a}_n$ ($n = 1, 2, 3, 4$) are the eigenvalues and corresponding column eigenvectors of $\bar{\bar{T}}$, respectively, and D_n are the amplitude coefficients. Furthermore, the transverse fields in Eq. (2) can be regarded as a superposition of four waves along the z direction, and the eigenvalues are the corresponding wavenumbers. Physically, these four waves can be further divided into two types of waves going along two opposite directions, respectively. As a result, Eq. (2) can be rewritten as

$$\mathbf{S}(z) = [\bar{\bar{a}}_+ \quad \bar{\bar{a}}_-] \begin{bmatrix} \exp(-j\bar{\bar{\lambda}}_+ z) & \\ & \exp(-j\bar{\bar{\lambda}}_- z) \end{bmatrix} \begin{bmatrix} \mathbf{D}_+ \\ \mathbf{D}_- \end{bmatrix}, \tag{3}$$

where $\bar{\bar{a}}_\pm$ is a 4×2 matrix, which includes two columns of the eigenvector matrix in Eq. (2), $\exp(-j\bar{\bar{\lambda}}_\pm z)$ is a 2×2 diagonal matrix composed of the two corresponding eigenvalues, and $\mathbf{D}_\pm$ is a 2×1 coefficient column vector. The subscript "+" involves the components "1" and "2" in Eq. (2), and refers to the waves along the $+z$ axis. The subscript "−" involves the components of "3" and "4," and represents the waves along the $-z$ axis.

According to the full wave analysis above, if surface waves exist at the $z = 0$ plane, as shown in Fig. 1, the transverse fields in both media become

$$\mathbf{S}^A(z) = \bar{\bar{a}}_+^A[\exp(-j\bar{\bar{\lambda}}_+^A z)]\mathbf{D}_+^A, \tag{4}$$

$$\mathbf{S}^B(z+d) = \bar{\bar{a}}_-^B \exp[-j\bar{\bar{\lambda}}_-^B(z+d)]\mathbf{D}_-^B + \bar{\bar{a}}_+^B \exp[-j\bar{\bar{\lambda}}_+^B(z+d)]\bar{\bar{R}}(-d)\mathbf{D}_-^B, \tag{5}$$

where the superscripts "A" and "B" represent the fields in media A and B, respectively. $\bar{\bar{R}}(-d)$ is the 2×2 reflection coefficient matrix at the $z = -d$ plane, as shown in Appendix B.

It is worth mentioning that the wave propagation state in each medium is determined by the corresponding eigenvalue. That is, the wave decays exponentially along the $\pm z$ direction when the eigenvalue is a purely imaginary number, while it propagates without decay when the eigenvalue is purely real. Moreover, it gives rise to an oscillation component of the electric field once the corresponding eigenvalue is a complex number. In practical designs, these eigenvalues are determined by the physical characteristics of the material, which mainly refer to the relative permittivity and permeability tensors.

Since surface waves are supported at the interface of medium A and medium B, as shown in Fig. 1, the boundary conditions should be in such a way that the transverse fields must be continuous across the interface plane. Combining Eqs. (4) and (5), the boundary conditions at the $z = 0$ plane can be obtained by

$$\det[\,\bar{\bar{a}}_+^A \quad \bar{\bar{a}}_+^B \exp(-j\bar{\bar{\lambda}}_+^B d)\bar{\bar{R}}(-d) + \bar{\bar{a}}_-^B \exp(-j\bar{\bar{\lambda}}_-^B d)\,] = 0. \tag{6}$$

In the following parts, a theoretical analysis is conducted to discuss the dispersion relation and other relevant characteristics of Dyakonov SWs existing in a conductor-backed structure.

B. Dyakonov SWs in a Conductor-Backed Structure

As shown in Fig. 1, the medium A ($z > 0$) is a semi-infinite isotropic medium with a relative permittivity ε_A. The medium

B ($-d < z < 0$) is a conductor-backed uniaxial birefringent slab with a relative permittivity tensor $\bar{\bar{\varepsilon}}_r \cdot \varepsilon_{or}$ and ε_{ex} are the ordinary and extraordinary relative permittivity scalars of $\bar{\bar{\varepsilon}}_r$, respectively. Dyakonov has proven that Dyakonov SWs can only be supported by satisfying the relationship $\varepsilon_{or} < \varepsilon_A < \varepsilon_{ex}$ [2]. The optic axis of the uniaxial medium lies at the interface ($z = 0$ plane) of two partnering media, and has an angle θ with respect to the propagation direction, as shown in Fig. 2. As a result, it is convenient to obtain the unit vector of the optic axis $\hat{c} = (\cos\theta, -\sin\theta, 0)^T$. The relative permittivity tensor [6] of the uniaxial substrate is

$$\bar{\bar{\varepsilon}}_r = \begin{bmatrix} \varepsilon_{ex}\cos^2\theta + \varepsilon_{or}\sin^2\theta & (\varepsilon_{or} - \varepsilon_{ex})\cos\theta\sin\theta & 0 \\ (\varepsilon_{or} - \varepsilon_{ex})\cos\theta\sin\theta & \varepsilon_{or}\cos^2\theta + \varepsilon_{ex}\sin^2\theta & 0 \\ 0 & 0 & \varepsilon_{or} \end{bmatrix}. \tag{7}$$

In the upper isotropic medium, the waves can be separated into TE and TM waves according to different polarization states. As Dyakonov SWs exist at the interface, the waves that exponentially decay along the $+z$ axis can be supported in the isotropic medium. The eigenvalues of these waves are

$$\lambda^A_{TE+} = \lambda^A_{TM+} = -(\varepsilon_A - \beta^2)^{1/2}, \tag{8}$$

where $\beta = p/k_0$ is the normalized propagation constant along the $+x$ direction, and the normalization factor k_0 is the free space wavenumber. The corresponding eigenvectors are given by

$$\mathbf{a}^A_{TE+} = \begin{bmatrix} 0 \\ 1 \\ -\lambda^A_{TE+} \\ 0 \end{bmatrix}, \qquad \mathbf{a}^A_{TM+} = \begin{bmatrix} \lambda^A_{TE+} \\ 0 \\ 0 \\ \varepsilon_A \end{bmatrix}. \tag{9}$$

In the lower uniaxial slab, the waves can be divided into ordinary waves and extraordinary waves. Unlike the upper medium, the waves in the slab include both incident waves and reflected waves. Therefore, the eigenvalues can be written as

$$\lambda^B_{ex\pm} = \mp[\varepsilon_{ex} - \beta^2(\varepsilon_{ex}\cos^2\theta + \varepsilon_{or}\sin^2\theta)/\varepsilon_{or}]^{1/2}, \tag{10}$$

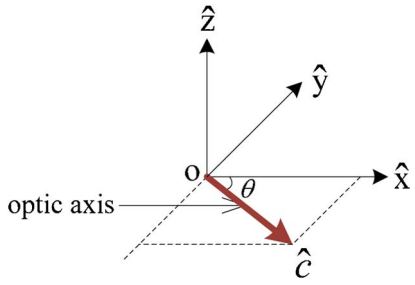

Fig. 2. Orientation of the optic axis $\hat{c}$ located at the interface ($z = 0$ plane) of both media and at an angle θ ($0 < \theta < \pi/2$) with the $+x$ axis.

$$\lambda^B_{or\pm} = \mp(\varepsilon_{or} - \beta^2)^{1/2}, \tag{11}$$

where the subscript "ex" means extraordinary waves and "or" means ordinary waves. The eigenvectors are determined by

$$\mathbf{a}^B_{ex\pm} = \begin{bmatrix} (\varepsilon_{or} - \beta^2)\cos\theta \\ -\varepsilon_{or}\sin\theta \\ \lambda^B_{ex\pm}\varepsilon_{or}\sin\theta \\ \lambda^B_{ex\pm}\varepsilon_{or}\cos\theta \end{bmatrix}, \qquad \mathbf{a}^B_{or\pm} = \begin{bmatrix} \lambda^B_{or\pm}\sin\theta \\ \lambda^B_{or\pm}\cos\theta \\ -(\lambda^B_{or\pm})^2\cos\theta \\ \varepsilon_{or}\sin\theta \end{bmatrix}. \tag{12}$$

In addition, according to Appendix B, the reflection coefficient matrix is calculated as

$$\bar{\bar{R}}(-d) = \begin{bmatrix} 1 & \\ & -1 \end{bmatrix}. \tag{13}$$

Assuming that Dyakonov SWs are supported at the interface plane, the electric and magnetic fields in both materials should exponentially decay away from the interface, and the corresponding eigenvalues should be purely imaginary. Let $\lambda^A_{TE+} = \lambda^A_{TM+} = -jq_1$, $\lambda^B_{ex\pm} = \mp jq_2$, $\lambda^B_{or\pm} = \mp jq_3$, where $q_m (m = 1, 2, 3)$ are positive values. By substituting Eqs. (8)–(13) into Eq. (6), the dispersion equation becomes

$$\begin{aligned} &q_1 q_3 \varepsilon_A (q_3^2 N - M)\tanh(q_2 k_0 d)\tanh(q_3 k_0 d) \\ &+ (q_3^4 \varepsilon_A N - q_1^2 \varepsilon_{or} M)\tanh(q_2 k_0 d) \\ &+ q_2 q_3 (q_1^2 \varepsilon_{or} N - \varepsilon_A M)\tanh(q_3 k_0 d) \\ &+ q_1 q_2 \varepsilon_{or}(q_3^2 N - M) = 0, \end{aligned} \tag{14}$$

where $N = (\varepsilon_{ex} - \varepsilon_A) + q_2^2 - q_1^2$ and $M = \varepsilon_{ex}(\varepsilon_A - \varepsilon_{or}) + q_1^2\varepsilon_{ex} - q_2^2\varepsilon_{or}$. Therefore, once the slab height d is given, the remaining parameter β can be solved. It should be mentioned that Eq. (14) will transform into a simplified expression, which is consistent with Dyakonov's work [2] when d is infinite.

3. NUMERICAL RESULTS AND DISCUSSION

In order to further understand the properties of Dyakonov SWs, which exist at the critical surface of a limited thickness structure, the effect of different heights on the characteristics of Dyakonov SWs is discussed in the following sections.

A. Angular Existence Domain

Equation (14) shows that the dispersion equation of Dyakonov SWs involves $q_m (m = 1, 2, 3)$ and d, when the permittivity scalars of both media are given. Consequently, the existence conditions of Dyakonov SWs are only determined by q_m, if the uniaxial medium has a finite thickness. Furthermore, Dyakonov SWs can be supported in a region, where q_m are positive real values. This region is known as the angular existence domain [11]. Figure 3 shows two pairs of q_m as a function of θ for $d = 3.5\lambda_0$ and $4.5\lambda_0$. A natural uniaxial material named liquid crystal E7 is considered for numerical calculation. This crystal material has an ordinary relative permittivity $\varepsilon_{or} = 1.520^2$ and an extraordinary relative permittivity $\varepsilon_{ex} = 1.725^2$. The relative permittivity of the isotropic medium is $\varepsilon_A = 1.569^2$. As shown in Fig. 3, the existence domain of Dyakonov SWs is located between these two black dashed–dotted/dashed lines, which are mainly determined by q_1 and q_2 for

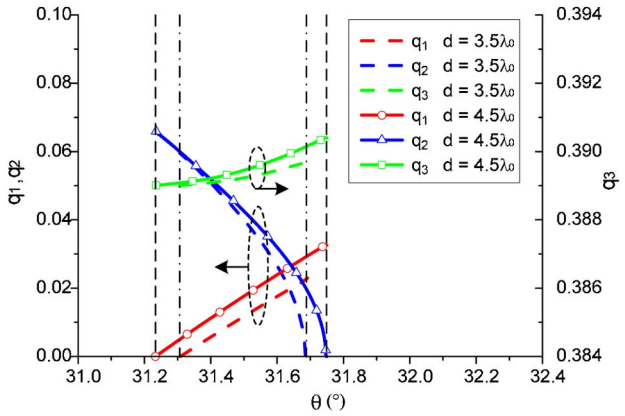

Fig. 3. $q_m(m = 1, 2, 3)$ as a function of θ when $d = 3.5\lambda_0$ and $d = 4.5\lambda_0$ ($\varepsilon_A = 1.569^2$, $\varepsilon_{or} = 1.520^2$, and $\varepsilon_{ex} = 1.725^2$). The black dashed–dotted/dashed lines represent the boundary values of the angular existence domain for $d = 3.5\lambda_0/4.5\lambda_0$, respectively.

a given thickness d. More specifically, the lower limit of the domain is determined by q_1, and the upper limit is determined by q_2. The value of q_3 has little effect on the domain, since it is always above zero. Compared with the cases $d = 4.5\lambda_0$ (solid lines) and $d = 3.5\lambda_0$ (dashed lines), the curves of q_m slightly shift down and the existence region becomes narrower. As shown in Fig. 3, the curve of q_1 shifts to the right and keeps on increasing almost linearly when d decreases. However, the curve of q_2 decreases more sharply and has a smaller value of the upper limit when d decreases. Compared with the curves of q_1 and q_2, the curve of q_3 keeps the same monotonicity and has a smaller slope when d changes. According to the analysis above, even if the slab has different heights, the minimum value of θ can still be calculated by Eq. (14) for $q_1 = 0$, while the maximum value of θ can be obtained when $q_2 = 0$.

The variation of the angular existence domain with an increase of d is shown in Fig. 4, where only the rainbow region can support Dyakonov SWs. It is obvious that the minimum height d_{min}, which is closely related to the existence of Dyakonov SWs, is determined by the point P. From this figure, we can obtain that the point P is the cross point of $q_1 = 0$ and $q_2 = 0$ curves. As a result, the minimum thickness d_{min} satisfies

$$[\tanh(Q)]/Q = (\varepsilon_{ex} - \varepsilon_A)/\varepsilon_{ex}, \tag{15}$$

where $Q = k_0 d_{min}(\varepsilon_A - \varepsilon_{or})^{1/2}$. Obviously, the minimum thickness of the slab is only affected by the relative permittivities of both materials. Moreover, the existence region increases with an increase of d, but both curves approach certain asymptotic lines (black dashed–dotted lines) when d is getting close to infinite. Here, these two black dashed–dotted lines can be calculated by equations in [2], where Dyakonov SWs existing at the interface of a semi-infinite structure are introduced. The upper boundary of this existence region can be obtained by substituting $q_2 = 0$ into Eq. (14), while the lower boundary is determined by Eq. (14) when $q_1 = 0$.

It is worth mentioning that Fig. 4 also shows the distribution of the normalized propagation constant β in the existence region of Dyakonov SWs. In this figure, the value of β has a small increase with the increase of the slab height in a certain direction within the existence region. For a given height, the value of β increases with the increase of the angle $\theta(0 < \theta < \pi/2)$. From Fig. 4, it can be observed that the value of β has a minimum value. And this value is determined by the conditions that $q_m(m = 1, 2, 3)$ must be above zero in the existence region of Dyakonov SWs.

Actually, it is inevitable that Dyakonov SWs will coexist with guided waves in this layered structure. It should be pointed out that Dyakonov SWs only exist within the existence domain, which locates at the interface of the isotropic medium and the uniaxial medium, as shown in Fig. 4. And guided waves can be supported both inside and outside of the domain range in the uniaxial layer. These two kinds of waves can be distinguished by their respective normalized wavenumbers, since the former has a normalized wavenumber always above the latter. In this paper, we mainly concentrated on the related information of Dyakonov SWs.

In fact, the internal relationship between the permittivities also has a severe impact on the existence region. Figure 5 shows that the angular difference $\Delta\theta$ varies with the thickness d for different values of ε_A when ε_{or} and ε_{ex} are fixed. Generally, the best value of ε_A is a little smaller than the

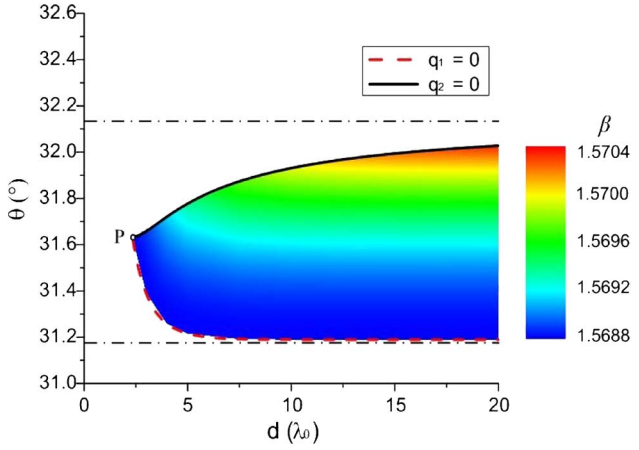

Fig. 4. Variations of angle θ and the normalized propagation constant β with respect to the increase of height d for $q_1 = 0$ and $q_2 = 0$. The point P is the critical point at which Dyakonov SWs can exist at a minimum height ($\varepsilon_A = 1.569^2$, $\varepsilon_{or} = 1.520^2$, and $\varepsilon_{ex} = 1.725^2$). The two black dashed–dotted lines are the boundary values of the angular existence domain when d is infinite.

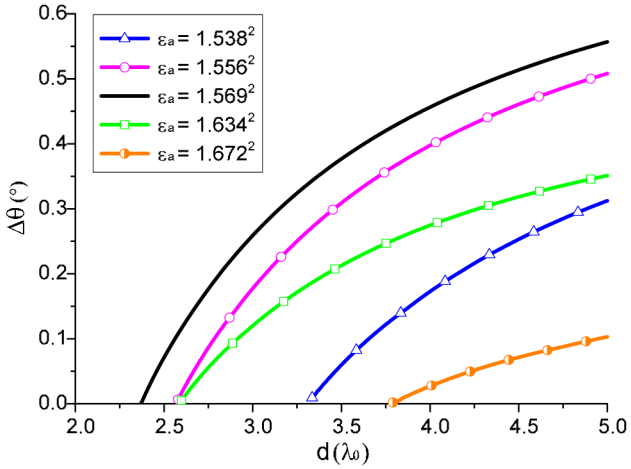

Fig. 5. Variations of the angular difference $\Delta\theta$ with respect to the increase of height d for $\varepsilon_A = 1.538^2$, 1.556^2, 1.569^2, 1.634^2, and 1.672^2 ($\varepsilon_{or} = 1.520^2$, $\varepsilon_{ex} = 1.725^2$).

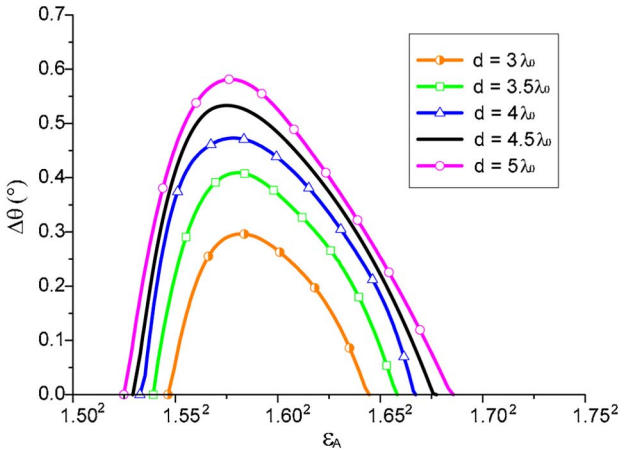

Fig. 6. Variations of the angular difference $\Delta\theta$ with respect to the increase of the relative permittivity ε_A for $d = 3\lambda_0$, $3.5\lambda_0$, $4\lambda_0$, $4.5\lambda_0$, and $5\lambda_0$ ($\varepsilon_{or} = 1.520^2$, $\varepsilon_{ex} = 1.725^2$).

middle value between ε_{or} and ε_{ex}, as displayed by the black solid line in the figure. At this value of ε_A, $\Delta\theta$ increases most rapidly with respect to the thickness d; in the meantime the corresponding cut-off thickness d_{min} has a minimum value. A detailed study regarding the change of the angular difference $\Delta\theta$ over the increase of ε_A for different heights is presented in Fig. 6. It is clearly shown that both the maximum value of $\Delta\theta$ and the range of tolerable ε_A increase as d increases. However, the variation tendency of the curve begins to slow down and the maximum value approaches a stable value eventually. This is reasonable since the reflected waves in the slab become weaker and the surface waves gradually turn out to be the initial case of Dyakonov SWs [2] when the thickness d keeps increasing. It is also proven that the value of ε_A is relatively closer to the ordinary permittivity ε_{or} than the extraordinary permittivity ε_{ex}, if the angular difference of the existence domain reaches a maximum value.

In conclusion, the existence region is very sensitive to the slab height and the relative permittivities of both media. Thus, Dyakonov SWs can be used in switching or sensing applications, which are highly dependent on the permittivities of the media [24,25].

B. Field Distributions

It has been proven that the transverse fields in a homogenous medium can be expressed by a combination of eigenvalues and eigenvectors, as discussed in Section 2.A. Therefore, the completed expressions of electric and magnetic fields in both media can be further derived by using Maxwell's equations. In the isotropic medium ($z > 0$), the electric and magnetic fields are in the form of

$$\mathbf{E}_{TE} = D_{TE}\begin{bmatrix}0\\1\\0\end{bmatrix}\exp(-q_1k_0z)\exp[j(\omega t-\beta k_0x)], \quad (16)$$

$$\mathbf{E}_{TM} = D_{TM}\begin{bmatrix}-jq_1\\0\\-\beta\end{bmatrix}\exp(-q_1k_0z)\exp[j(\omega t-\beta k_0x)], \quad (17)$$

$$\mathbf{H}_{TE} = \frac{D_{TE}}{\eta_0}\begin{bmatrix}jq_1\\0\\\beta\end{bmatrix}\exp(-q_1k_0z)\exp[j(\omega t-\beta k_0x)], \quad (18)$$

$$\mathbf{H}_{TM} = \frac{D_{TM}}{\eta_0}\begin{bmatrix}0\\\varepsilon_A\\0\end{bmatrix}\exp(-q_1k_0z)\exp[j(\omega t-\beta k_0x)]. \quad (19)$$

In the conductor-backed uniaxial slab ($-d < z < 0$), the electric and magnetic fields are

$$\mathbf{E}_{or} = D_{or}\begin{bmatrix}jq_3\sin\theta\sinh[q_3k_0(z+d)]\\jq_3\cos\theta\sinh[q_3k_0(z+d)]\\-\beta\sin\theta\cosh[q_3k_0(z+d)]\end{bmatrix}\exp[j(\omega t-\beta k_0x)], \quad (20)$$

$$\mathbf{E}_{ex} = D_{ex}\begin{bmatrix}(\varepsilon_{or}-\beta^2)\cos\theta\sinh[q_2k_0(z+d)]\\-\varepsilon_{or}\sin\theta\sinh[q_2k_0(z+d)]\\-jq_2\beta\cos\theta\cosh[q_2k_0(z+d)]\end{bmatrix}\exp[j(\omega t-\beta k_0x)], \quad (21)$$

$$\mathbf{H}_{or} = \frac{D_{or}}{\eta_0}\begin{bmatrix}q_3^2\cos\theta\cosh[q_3k_0(z+d)]\\\varepsilon_{or}\sin\theta\cosh[q_3k_0(z+d)]\\jq_3\beta\cos\theta\sinh[q_3k_0(z+d)]\end{bmatrix}\exp[j(\omega t-\beta k_0x)], \quad (22)$$

$$\mathbf{H}_{ex} = \frac{D_{ex}}{\eta_0}\begin{bmatrix}jq_2\varepsilon_{or}\sin\theta\cosh[q_2k_0(z+d)]\\jq_2\varepsilon_{or}\cos\theta\cosh[q_2k_0(z+d)]\\-\varepsilon_{or}\beta\sin\theta\sinh[q_2k_0(z+d)]\end{bmatrix}\exp[j(\omega t-\beta k_0x)], \quad (23)$$

where D_{TE}, D_{TM}, D_{or}, and D_{ex} are the unknown amplitudes of the fields.

Figure 7 shows the transverse electric-field distributions of Dyakonov SWs along the z direction. The field distributions in the uniaxial slab are more complicated, compared with those in the isotropic medium. In the uniaxial slab, the total waves (blue lines) include four components, i.e., the ordinary and extraordinary components of incident waves, and the counterparts of reflected waves. For the incident waves, the values of ordinary and extraordinary components have opposite signs. The ordinary component decays away from the interface much faster than its extraordinary counterpart due to the differences between the eigenvalues. As a result, the ordinary component of the reflected waves is very weak and can be ignored in this structure. It is seen that the phenomenon of the peaks of the total waves in the slab slightly shifting from the interface ($z = 0$ plane) is mainly caused by the different slopes of the ordinary and extraordinary waves' curves. The amplitude distributions of the Ey component have similar variation trends except that the maximum amplitude is almost

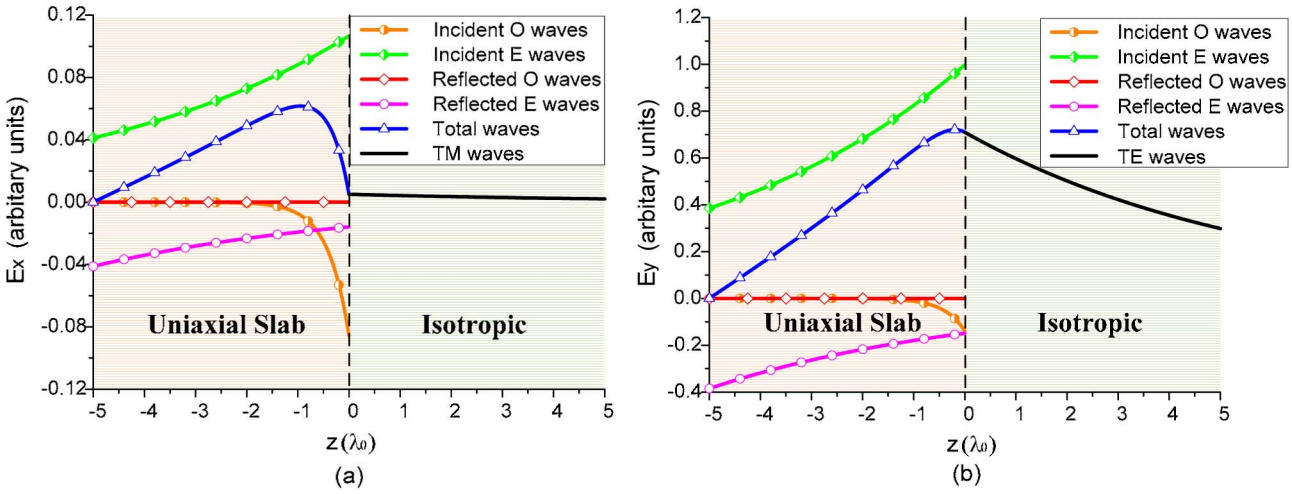

Fig. 7. Amplitude distributions of the transverse electric-field components in two partnering media for (a) amplitude of Ex component and (b) amplitude of Ey component. "O" and "E" waves denote ordinary and extraordinary waves, respectively. In this condition ($\varepsilon_A = 1.569^2$, $\varepsilon_{or} = 1.520^2$, $\varepsilon_{ex} = 1.725^2$, and $d = 5\lambda_0$), the angular existence domain is $\Delta\theta = 0.557°$. The angle between the optic axis and the propagation direction is $\theta = 31.63°$, which corresponds to the location of point P.

tenfold over the Ex component, which verifies that Dyakonov SWs are TE-dominant hybrid waves.

C. Other Finite Thickness Structures

As a matter of fact, the method introduced in this paper can be regarded as a generalized analysis method for other finite thickness structures. The relevant equations and expressions can be obtained by appropriately selecting eigenvalues, eigenvectors, and the reflection coefficient matrix.

For the analyzed isotropic-uniaxial-PEC configuration (the optic axis of the uniaxial slab lies at the interface plane), the reflection coefficient matrix is in a diagonal form, as shown in Eq. (13). Accordingly, the ordinary or extraordinary component of the reflected waves is completely determined by the counterpart of the incident waves. However, in the case in which the optic axis of the uniaxial medium has an inclination angle with the interface plane, the eigenvalues and eigenvectors will be complicated. Partial eigenvalues will become complex numbers, and the reflection coefficient matrix will turn out to be a matrix with four nonzero elements. This means that the ordinary or extraordinary component of the reflected waves will come from both ordinary and extraordinary components of the incident waves [21].

In addition, the relevant equations and expressions of other similar structures can be obtained by using this analytical method. If we take the uniaxial-isotropic-PEC (the optic axis lies at the interface plane) one as an example, the solving process is very similar except for interchanging the relevant eigenvalues and eigenvectors of two media. Compared with the introduced case, this reversed structure may have a lot of analogous properties, such as the existence of cut-off thickness, and variation of the existence range.

It is worthwhile to mention that, instead of PEC, this generalized analysis method is also applicable to the real conductor cases. Different from the PEC structures, the boundary conditions at the surface plane of the real conductor should take the losses into account. Therefore, the expressions of the reflection coefficient matrix will be different, as shown in Appendix B. Due to the existence of surface resistances, all four of these elements of the reflection coefficient matrix will become complex numbers. Meanwhile, the remaining solving process of the characteristic equation is nearly the same.

4. CONCLUSIONS

In this paper, Dyakonov SWs propagating at the interface of an isotropic medium and a conductor-backed uniaxial birefringent slab have been analyzed using the exponential-matrix method. Based on the obtained dispersion equation, the minimum thickness d_{min} of the slab can be expressed and calculated. It is found that the existence region of Dyakonov SWs in a finite structure is always smaller than that of the ideal semi-infinite media structure. However, as long as the thickness d is above the minimum value d_{min}, the existence region will become wider and wider when d keeps increasing. Finally, the region scope of Dyakonov SWs will tend to be quite close to the scope of the case with semi-infinite thickness. As a result, a trade-off between a desired existence area and a tolerable thickness should be made for a practical design of Dyakonov SWs. Furthermore, in order to get the widest existence area at a certain thickness, the relative permittivity of the isotropic medium should be carefully selected.

It is demonstrated that the distribution of the propagation constant is seriously affected by the slab thickness. For a given height, the propagation constant β increases with the increase of the angle between the optic axis direction and the wave propagation direction. In addition, the electric- and magnetic-field distributions of two media are also shown in this paper. It can be seen that the transverse electric-field components of ordinary waves have opposite signs with the extraordinary counterparts in the uniaxial medium. The ordinary component of the incident waves decays away from the interface much faster than the extraordinary counterpart. It is noteworthy that this method can be regarded as a generalized analysis method to analyze the properties of Dyakonov SWs in other similar finite structures.

In conclusion, Dyakonov SWs existing at an isotropic-uniaxial-PEC structure have great potential in practical switching or sensing applications, since the existence domain is highly sensitive to the slab's height and permittivities of the

two partner media. The analysis method introduced in this paper has more advantages in analyzing and utilizing this kind of surface wave existing at different kinds of finite thickness structures.

APPENDIX A: COEFFICIENT MATRIX $\bar{\bar{T}}$

For a homogeneous anisotropic medium, the coefficient matrix $\bar{\bar{T}}$ in Eq. (1) is

$$\bar{\bar{T}}=\begin{bmatrix} -\frac{\varepsilon_{zx}}{\varepsilon_{zz}}p & p\left(\frac{\mu_{yz}}{\mu_{zz}}-\frac{\varepsilon_{zy}}{\varepsilon_{zz}}\right) & k_0\left(\mu_{yx}-\frac{\mu_{zx}\mu_{yz}}{\mu_{zz}}\right) & -\frac{p^2}{k_0\varepsilon_{zz}}+k_0\left(\mu_{yy}-\frac{\mu_{zy}\mu_{yz}}{\mu_{zz}}\right) \\ 0 & -\frac{\mu_{xz}}{\mu_{zz}}p & k_0\left(\frac{\mu_{zx}\mu_{xz}}{\mu_{zz}}-\mu_{xx}\right) & k_0\left(\frac{\mu_{zy}\mu_{xz}}{\mu_{zz}}-\mu_{xy}\right) \\ k_0\left(\frac{\varepsilon_{yz}\varepsilon_{zx}}{\varepsilon_{zz}}-\varepsilon_{yx}\right) & \frac{p^2}{k_0\mu_{zz}}+k_0\left(\frac{\varepsilon_{yz}\varepsilon_{zy}}{\varepsilon_{zz}}-\varepsilon_{yy}\right) & -\frac{\mu_{zx}}{\mu_{zz}}p & p\left(\frac{\varepsilon_{yz}}{\varepsilon_{zz}}-\frac{\mu_{zy}}{\mu_{zz}}\right) \\ k_0\left(\varepsilon_{xx}-\frac{\varepsilon_{xz}\varepsilon_{zx}}{\varepsilon_{zz}}\right) & k_0\left(\varepsilon_{xy}-\frac{\varepsilon_{xz}\varepsilon_{zy}}{\varepsilon_{zz}}\right) & 0 & -\frac{\varepsilon_{xz}}{\varepsilon_{zz}}p \end{bmatrix}, \tag{A1}$$

where p is the propagation constant along the $+x$ direction, k_0 is the free space wavenumber, and ε_{ij} and $\mu_{ij}(i,j=x,y,z)$ are the corresponding elements of the relative permittivity and permeability tensors, respectively.

APPENDIX B: REFLECTION COEFFICIENT MATRIX $\bar{\bar{R}}$

According to Eq. (2), the transverse field distribution in medium B can be written as

$$\mathbf{S}^B(z+d)=\sum_{n=1}^{4}\mathbf{a}_n\ \exp[-j\lambda_n(z+d)]D_n. \tag{B1}$$

If the $z=-d$ plane is a PEC plane, the transverse electric field in Eq. (B1) should satisfy

$$\begin{aligned} &a_{11}D_1+a_{12}D_2+a_{13}D_3+a_{14}D_4=0,\\ &a_{21}D_1+a_{22}D_2+a_{23}D_3+a_{24}D_4=0, \end{aligned} \tag{B2}$$

where $a_{ij}(i,j=1,2)$ is the ith element of the eigenvector $\mathbf{a}_j$, and the analysis above does not take the secondary reflection into account. To simplify these equations, Eq. (B2) can be written as

$$\begin{bmatrix} D_1 \\ D_2 \end{bmatrix}=\begin{bmatrix} R_{11} & R_{12} \\ R_{21} & R_{22} \end{bmatrix}\begin{bmatrix} D_3 \\ D_4 \end{bmatrix}, \tag{B3}$$

where $R_{11}=(a_{12}a_{23}-a_{13}a_{22})/M$, $R_{12}=(a_{12}a_{24}-a_{14}a_{22})/M$, $R_{21}=(a_{13}a_{21}-a_{11}a_{23})/M$, $R_{22}=(a_{14}a_{21}-a_{11}a_{24})/M$, and $M=a_{11}a_{22}-a_{12}a_{21}$. As shown in Fig. 1, D_1 and D_2 refer to the amplitude coefficients of the reflected waves in medium B, while D_3 and D_4 refer to the amplitude coefficients of the incident waves. Therefore, the reflection coefficient matrix at the $z=-d$ plane is

$$\bar{\bar{R}}(-d)=\begin{bmatrix} R_{11} & R_{12} \\ R_{21} & R_{22} \end{bmatrix}. \tag{B4}$$

If the $z=-d$ plane is a real conductor plane, the fields should satisfy the standard impedance boundary condition (SIBC), i.e., $\hat{z}\times(\hat{z}\times\mathbf{E})=-Z_s(\hat{z}\times\mathbf{H})$, where Z_s is the surface resistance of the lossy conductor. As a consequence, the transverse electric field in Eq. (B1) should satisfy

$$\begin{aligned} &a_{11}D_1+a_{12}D_2+a_{13}D_3+a_{14}D_4\\ &\quad=-Z_s(a_{41}D_1+a_{42}D_2+a_{43}D_3+a_{44}D_4),\\ &a_{21}D_1+a_{22}D_2+a_{23}D_3+a_{24}D_4\\ &\quad=Z_s(a_{31}D_1+a_{32}D_2+a_{33}D_3+a_{34}D_4). \end{aligned} \tag{B5}$$

To simplify them, Eq. (B5) becomes

$$\begin{bmatrix} D_1 \\ D_2 \end{bmatrix}=\begin{bmatrix} R\prime_{11} & R\prime_{12} \\ R\prime_{21} & R\prime_{22} \end{bmatrix}\begin{bmatrix} D_3 \\ D_4 \end{bmatrix}, \tag{B6}$$

where $R'_{11}=[(a_{12}+Z_sa_{42})(a_{23}-Z_sa_{33})-(a_{13}+Z_sa_{43})(a_{22}-Z_sa_{32})]/M$, $R'_{12}=[(a_{12}+Z_sa_{42})(a_{24}-Z_sa_{34})-(a_{14}+Z_sa_{44})(a_{22}-Z_sa_{32})]/M$, $R'_{21}=[(a_{13}+Z_sa_{43})(a_{21}-Z_sa_{31})-(a_{11}+Z_sa_{41})(a_{23}-Z_sa_{33})]/M$, $R'_{22}=[(a_{14}+Z_sa_{44})(a_{21}-Z_sa_{31})-(a_{11}+Z_sa_{41})(a_{24}-Z_sa_{34})]/M$, and $M=(a_{11}+Z_sa_{41})(a_{22}-Z_sa_{32})-(a_{12}+Z_sa_{42})(a_{21}-Z_sa_{31})$.

Therefore, the reflection coefficient matrix at a real conductor plane can be written as

$$\bar{\bar{R}}\prime(-d)=\begin{bmatrix} R'_{11} & R'_{12} \\ R'_{21} & R'_{22} \end{bmatrix}. \tag{B7}$$

ACKNOWLEDGMENTS

The authors are grateful to Osamu Takayama, David Artigas at ICFO–Institut de Ciencies Fotoniques, Mediterranean Technology Park, Barcelona, Spain, and John A. Polo Jr. at the Department of Chemistry and Physics, Edinboro University of Pennsylvania, Pennsylvania, USA, for their helpful discussions. We also appreciate the reviewers for their very thoughtful comments, which definitely improved the quality of this paper.

REFERENCES

1. J. Zenneck, "Über die Fortpflanzung ebener elektromagnetischer Wellen längs einer ebenen Lieterfläche und ihre Beziehung zur drahtlosen Telegraphie," Ann. Phys. Lpz. **23**, 846–866 (1907).

2. M. I. Dyakonov, "New type of electromagnetic wave propagating at an interface," Sov. Phys. JETP **67**, 714–716 (1988).
3. N. S. Averkiev and M. I. Dyakonov, "Electromagnetic waves localized at the interface of transparent anisotropic media," Opt. Spectrosc. **68**, 653–655 (1990).
4. D. B. Walker, E. N. Glytsis, and T. K. Gaylord, "Surface mode at isotropic-uniaxial and isotropic-biaxial interfaces," J. Opt. Soc. Am. A **15**, 248–260 (1998).
5. M. A. Morgan, D. L. Fisher, and E. A. Milne, "Electromagnetic scattering by stratified inhomogeneous anisotropic media," IEEE Trans. Antennas Propag. **35**, 191–197 (1987).
6. J. A. Polo Jr., S. Nelatury, and A. Lakhtakia, "Surface electromagnetic wave at a tilted uniaxial bicrystalline interface," Electromagnetics **26**, 629–642 (2006).
7. S. R. Nelatury, J. A. Polo Jr., and A. Lakhtakia, "Surface waves with simple exponential transverse decay at a biaxial bicrystalline interface," J. Opt. Soc. Am. A **24**, 856–865 (2007).
8. J. A. Polo Jr., S. R. Nelatury, and A. Lakhtakia, "Surface waves at a biaxial bicrystalline interface," J. Opt. Soc. Am. A **24**, 2974–2979 (2007).
9. S. R. Nelatury, J. A. Polo Jr., and A. Lakhtakia, "Electrical control of surface-wave propagation at the planar interface of a linear electro-optic material and an isotropic dielectric material," Electromagnetics **28**, 162–174 (2008).
10. J. A. Polo Jr., S. R. Nelatury, and A. Lakhtakia, "Propagation of surface waves at the planar interface of a columnar thin film and an isotropic substrate," J. Nanophoton. **1**, 1–11 (2007).
11. O. Takayama, L. Crasovan, S. K. Johansen, D. Mihalache, D. Artigas, and L. Torner, "Dyakonov surface waves: a review," Electromagnetics **28**, 126–145 (2008).
12. O. Takayama, L. Crasovan, D. Artigas, and L. Torner, "Observation of Dyakonov surface waves," Phys. Rev. Lett. **102**, 043903 (2009).
13. O. Takayama, A. Y. Nikitin, L. Martin-Moreno, L. Torner, and D. Artigas, "Dyakonov surface wave resonant transmission," Opt. Express **19**, 6339–6347 (2011).
14. O. Takayama, D. Artigas, and L. Torner, "Practical dyakonons," Opt. Lett. **37**, 4311–4313 (2012).
15. O. Takayama, D. Artigas, and L. Torner, "Coupling plasmons and dyakonons," Opt. Lett. **37**, 1983–1985 (2012).
16. W. Shu and J. M. Song, "Complete mode spectrum of a grounded dielectric slab with double negative metamaterials," Progress Electromagn. Res. **65**, 103–123 (2006).
17. M. M. B. Suwailiam and Z. Chen, "Surface waves on a grounded double-negative (DNG) slab waveguide," Microw. Opt. Technol. Lett. **44**, 494–498 (2005).
18. P. Baccarelli, P. Burghignoli, F. Frezza, A. Galli, P. Lampariello, G. Lovat, and S. Paulotto, "Fundamental modal properties of surface waves on metamaterial grounded slabs," IEEE Trans. Microwave Theor. Tech. **53**, 1431–1442 (2005).
19. S. H. Liu, L. Chen, and C. H. Liang, "Guided modes in a grounded slab waveguide of uniaxially anisotropic lefthanded material," Microw. Opt. Technol. Lett. **49**, 1644–1648 (2007).
20. S. Mirhadi and M. K. Hessari, "Surface waves suppression in a biaxially anisotropic metamaterial," in *Proceedings of Progress In Electromagnetics Research Symposium* (2009), pp. 73–78.
21. A. Knoesen, T. K. Gaylord, and M. G. Moharam, "Hybrid guided modes in uniaxial dielectric planar waveguides," J. Lightwave Technol. **6**, 1083–1104 (1988).
22. T. A. Maldonado and T. K. Gaylord, "Hybrid guided modes in biaxial planar waveguides," J. Lightwave Technol. **14**, 486–499 (1996).
23. H. Y. Yang, J. Castaneda, and N. Alexopoulos, "Surface wave modes of printed circuits on ferrite substrates," IEEE Trans. Microwave Theor. Tech. **40**, 613–621 (1992).
24. L. Torner, J. P. Torres, F. Lederer, D. Mihalache, D. M. Baboiu, and M. Ciumac, "Nonlinear hybrid waves guided by birefringent interfaces," Electron. Lett. **29**, 1186–1188 (1993).
25. L. Torner, J. P. Torres, and D. Mihalache, "New type of guided waves in birefringent media," IEEE Photon. Technol. Lett. **5**, 201–203 (1993).